Vol 18 No 12, December 2009
1674-1056/2009/18(12)/5437-06

Chinese Physics B

© 2009 Chin. Phys. Soc.
and IOP Publishing Ltd

Screening influence on the Stark effect of impurity states in strained wurtzite GaN/$Al_xGa_{1-x}N$ heterojunctions under pressure*

Zhang Min(张 敏)[a)b)] and Ban Shi-Liang(班士良)[a)†]

[a)] *Department of Physics, School of Physical Science and Technology, Inner Mongolia University, Hohhot* 010021, *China*
[b)] *College of Physics and Electron Information, Inner Mongolia Normal University, Hohhot* 010022, *China*

(Received 22 August 2008; revised manuscript received 13 August 2009)

The screening effect of the random-phase-approximation on the states of shallow donor impurities in free strained wurtzite GaN/$Al_xGa_{1-x}N$ heterojunctions under hydrostatic pressure and an external electric field is investigated by using a variational method and a simplified coherent potential approximation. The variations of Stark energy shift with electric field, impurity position, Al component and areal electron density are discussed. Our results show that the screening dramatically reduces both the blue and red shifts as well as the binding energies of impurity states. For a given impurity position, the change in binding energy is more sensitive to the increase in hydrostatic pressure in the presence of the screening effect than that in the absence of the screening effect. The weakening of the blue and red shifts, induced by the screening effect, strengthens gradually with the increase of electric field. Furthermore, the screening effect weakens the mixture crystal effect, thereby influencing the Stark effect. The screening effect strengthens the influence of energy band bending on binding energy due to the areal electron density.

Keywords: strained wurtzite heterojunction, Stark effect, screening, pressure
PACC: 7155G, 7340L, 7320D, 3260S

1. Introduction

Semiconductors of III–V group hexagonal wurtzite nitrides, as promising candidates, have attracted significant attention due to their applications in optical, optoelectronic and electronic devices. Compared with the zinc-blende structure, the wurtzite crystal structure has a different unit-cell as well as a lower symmetry, which results in a large strain effect and thus in some abnormal properties. Many authors have studied the electronic and optical properties of strained heterostructures made from wurtzite nitrides.[1−3]

High pressure is one of the important methods to modulate the physical properties of strained materials. The optical properties of semiconductor heterostructures under hydrostatic pressure have been extensively studied. The effect of nonlinear piezoelectricity on the pressure coefficient of the light emission in (111)-oriented InGaAs/GaAs quantum wells was studied by Łepkowski.[4] Wagner *et al* [5] studied the pressure dependence of the dielectric and lattice-dynamical properties of GaN and AlN. In our previous papers,[6,7] the Stark effects of donor impurity states in strained zinc-blende and wurtzite nitride heterojunctions under pressure were discussed by neglecting the screening effect of the Coulombic potential on impurity states.

In the present paper, the effect of screened Coulombic potential on the states of shallow donor impurities in free strained wurtzite GaN/$Al_xGa_{1-x}N$ heterojunctions under hydrostatic pressure and an external electric field is investigated. A variational approach is adopted to obtain the binding energies, and a simplified coherent potential approximation[8] (SCPA) is extended to obtain some physical parameters of a ternary mixed crystal of wurtzite nitrides in the III–V group since its properties are more similar to those of a crystal of the II–VI group. The rest of the present paper is organized as follows. In Section 2, the theoretical method is described. The pressure and the strain dependence of the physics parameters used in our calculation are presented in Section 3. In Section 4, the results and a discussion are presented. Finally, some conclusions are drawn from the present study in Section 5.

*Project supported by the National Natural Science Foundation of China (Grant No 60566002), and the Specialized Research Fund for the Doctoral Program of Higher Education of China (Grant No 20070126001).
†Corresponding author. E-mail: slban@imu.edu.cn

2. Theoretical method

We consider a free strained wurtzite $GaN/Al_xGa_{1-x}N$ heterojunction whose channel side GaN, denoted by material 1, is located at $z > 0$ and barrier side $Al_xGa_{1-x}N$, denoted by material 2, is located at $z < 0$. The interface of the heterojunction is defined as the x–y plane. The Hamiltonian of the system including Thomas–Fermi screening to the Coulombic interaction between an impurity located at (0, 0, z_0) and an electron with charge of $-e$ at coordinates (x, y, z) can by written as

$$H = H_{\rm e} + H_{\rm c}, \tag{1}$$

where

$$H_{\rm e} = \left(\frac{p_\perp^2}{2m_{\perp 1}} + \frac{p_z^2}{2m_{z1}}\right)\theta(z) + \left(\frac{p_\perp^2}{2m_{\perp 2}} + \frac{p_z^2}{2m_{z2}}\right) \times \theta(-z) + V(z) + eFz, \tag{2}$$

and

$$H_{\rm c} = -\frac{e^2}{\kappa(z, z_0)[x^2 + y^2 + (z - z_0)^2]^{1/2}} f(r). \tag{3}$$

In Eq.(2), $p_\perp$ and p_z are the momenta of the electron in the x–y plane and the z direction, respectively. $m_{\perp\lambda}$ and $m_{z\lambda}$ are the material-dependent effective masses of the electron with $\lambda = 1, 2$. $\theta(\pm z)$ is the step function. $V(z)$ and F are the interface potential and an external electric field felt by the electron.[7] In Eq.(3), $\kappa(z, z_0)$ are the dielectric constants, and $f(r)$ is the screening factor which has been discussed in Refs.[9] and [10]. After a two-dimensional (2D) Fourier transformation in the random-phase-approximation, $\kappa(z, z_0)$ can be described by

$$\kappa(Q) = 1 + \frac{2}{a_{\rm B}Q} G(Q)F(Q), \tag{4}$$

where $a_{\rm B}$ is the effective Bohr radius and Q is the 2D wave vector. $G(Q)$ is defined as

$$G(Q) = \begin{cases} 1 & \text{for} \quad Q < 2Q_{\rm F}, \\ 1 - [1 - (2Q_{\rm F}/Q)^2]^{1/2} & \text{for} \quad Q > 2Q_{\rm F}, \end{cases} \tag{5}$$

in which the finite size of the Fermi surface with Fermi wave vector $Q_{\rm F} = (2\pi N_S)^{1/2}$ is taken into account. The screening factor $F(Q)$ satisfies

$$F(Q) = \iint {\rm d}z{\rm d}z' \left|\xi(z)\right|^2 {\rm e}^{-Q|z-z'|} \left|\xi(z')\right|^2. \tag{6}$$

Introducing variational parameters b, d, γ and normalization constants B, D, β, the trial wave function for the system can be chosen as[11]

$$\psi(x, y, z) = \varphi(x, y)\xi(z) = \varphi(\rho)\xi(z) \tag{7}$$

with

$$\varphi(\rho) = \left[\frac{1}{2\pi}\right]^{1/2} \gamma {\rm e}^{{\rm i}\boldsymbol{k}\cdot\boldsymbol{\rho}} {\rm e}^{-\gamma\rho/2}, \tag{8}$$

and

$$\xi(z) = \begin{cases} \xi_1(z) = Bb^{1/2}(bz + \beta){\rm e}^{-bz/2} & z > 0, \\ \xi_2(z) = Dd^{1/2}{\rm e}^{dz/2} & z < 0. \end{cases} \tag{9}$$

The variational energy of the impurity state at ground state can be obtained as

$$\begin{aligned} E(b, d) &= \langle\psi|\left(H_{\rm e} + H_z + H_{\rm c}\right)|\psi\rangle \\ &= E_{\rm e} + \langle T\rangle + \langle V_0\rangle + \langle V_d\rangle + \langle V_s\rangle \\ &\quad + E_{\rm ext} + E_{\rm c}, \end{aligned} \tag{10}$$

where $E_{\rm e}$, $\langle T\rangle$, $\langle V_0\rangle$, $\langle V_d\rangle$, $\langle V_s\rangle$ and $E_{\rm ext}$ were also given in Ref.[7]. In Eq.(10),

$$\begin{aligned} E_{\rm c} &= -\langle\psi|H_{\rm c}|\psi\rangle \\ &= -e^2\gamma^3 \int_0^\infty {\rm d}Q \frac{1}{(\gamma^2 + Q^2)^{3/2}} \langle\xi(z)| \frac{1}{\kappa(z, z_0)\kappa(Q)} \\ &\quad \times \exp(-|z - z_0|\,Q)\,|\xi(z)\rangle. \end{aligned} \tag{11}$$

Minimizing $E(b, d) - \langle V_s\rangle/2$ with respect to the variational parameters, one can obtain the ground state energy $E_{\rm g}$ of an impurity state.

If we let Eq.(3) be equal to zero and replace Eq.(5) by $\varphi(\rho) = {\rm e}^{{\rm i}\boldsymbol{k}\cdot\boldsymbol{\rho}}/\sqrt{2\pi\hbar}$, the ground state energy $E_{\rm f}$ for a free electron energy can be also derived in the same way. Then, the binding energy of the impurity state can be written as

$$E_{\rm B}(F) = E_{\rm f}(F) - E_{\rm g}(F). \tag{12}$$

The Stark energy shift of the impurity state is

$$\Delta E = E_{\rm B}(F) - E_{\rm B}(0). \tag{13}$$

3. Pressure and strain dependence of physical parameters

Under hydrostatic pressure P, the relationship between the components of uniaxial and biaxial strain tensors is $\varepsilon_{zz,i} = R^{\rm H}\varepsilon_{xx,i}$[12] with coefficient

$$R^{\rm H} = \frac{C_{11,i}(P) + C_{12,i}(P) - 2C_{13,i}(P)}{C_{33,i}(P) - C_{13,i}(P)} \quad (i = 1, 2), \tag{14}$$

where $C_{\alpha\beta,\,i}(P)$ is the pressure-dependent elastic constant for wurtzite nitrides and satisfies

$$C_{\alpha\beta,\,i}(P) = C_{\alpha\beta,\,i}(0) + \gamma_{\alpha\beta,\,i}P + \delta_{\alpha\beta,\,i}P^2. \quad (15)$$

In Eq.(15), coefficients $\gamma_{\alpha\beta,\,i}$ and $\delta_{\alpha\beta,\,i}$ were given in Ref.[13].

In a GaN/$Al_xGa_{1-x}N$ real heterojunction, the biaxial lattice-mismatch-induced strain is given as

$$\varepsilon_{xx,\,1} = \varepsilon_{yy,\,1} = \frac{a_2(P) - a_1(P)}{a_1(P)},$$
$$\varepsilon_{xx2} = \varepsilon_{yy2} = \frac{a_1(P) - a_2(P)}{a_2(P)}, \quad (16)$$

where the lattice constant dependence of hydrostatic pressure[14] is

$$a_i(P) = a_i(0)\left(1 - \frac{P}{3B_{0,\,i}(P)}\right) \quad (i = 1, 2). \quad (17)$$

The strain-dependent energy gaps of GaN and AlN are[15]

$$E_{g,\,\mathrm{GaN}}(P, \overleftrightarrow{\varepsilon}) = E_{g,\,\mathrm{GaN}}(P) + 2(a_{1,\,\mathrm{GaN}} + b_{1,\,\mathrm{GaN}})\varepsilon_{xx,\,\mathrm{GaN}} + (a_{2,\,\mathrm{GaN}} + b_{2,\,\mathrm{GaN}})\varepsilon_{zz,\,\mathrm{GaN}}, \quad (18)$$

and

$$E_{g,\,\mathrm{AlN}}(P, \overleftrightarrow{\varepsilon}) = E_{g,\,\mathrm{AlN}}(P) + 2a_{1,\,\mathrm{AlN}}\varepsilon_{xx,\,\mathrm{AlN}} + a_{2,\,\mathrm{AlN}}\varepsilon_{zz,\,\mathrm{AlN}}, \quad (19)$$

where the pressure-dependent energy gaps can be written as[16]

$$E_{\mathrm{g},\,i}(p) = E_{\mathrm{g},\,i}(0) + \alpha_i P + \beta_i P^2. \quad (20)$$

The energy gap of $Al_xGa_{1-x}N$ can be calculated in the SCPA[8] from

$$E_{\mathrm{TMC}} = \frac{E_{\mathrm{A}}E_{\mathrm{B}}}{xE_{\mathrm{A}} + (1-x)E_{\mathrm{B}}}. \quad (21)$$

The ratio of the conduction band to valence band offset is given as 65:20 in the strained wurtzite nitride quantum well.[17]

The biaxial, uniaxial and hydrostatic pressure dependence of the effective mass[18] in the z direction and the x–y plane of the electron can be calculated from

$$\frac{m^0_{i,\,\alpha\alpha}}{m_{i,\,\alpha\alpha}(P)} = 1 + \frac{C_i}{E_{\mathrm{g},\,i}(P)} \quad (i = 1, 2; \quad \alpha = x, z), \quad (22)$$

where C_i is a fixed value for a given material with $P = 0$. The effective mass of $Al_xGa_{1-x}N$ can be obtained by the linear interpolation method.

The tensor components of the static dielectric constant κ_0 in a wurtzite structure are derived from a generalized Lyddane–Sachs–Teller relation

$$\kappa_{0,\,\alpha\alpha} = \kappa_{\infty,\,\alpha\alpha}\left(\frac{\omega_{\mathrm{LO},\,\alpha\alpha}}{\omega_{\mathrm{TO},\,\alpha\alpha}}\right)^2 \quad (\alpha = x, z), \quad (23)$$

The frequencies of longitudinal optical (LO)- and transverse optical (TO)-phonons affected by strain can be written as[12]

$$\omega_{j,\,\alpha\alpha} = \omega_{j,\,\alpha\alpha}(0) + 2K_{j,\,\parallel}\varepsilon_{\parallel} + K_{j,\,\perp}\varepsilon_{\perp} \quad (j = A_1, E_1), \quad (24)$$

where $K_{j,\parallel}$ and $K_{j,\perp}$ are the strain coefficients related to the deformation potential of phonon modes.

Furthermore, the hydrostatic pressure dependence of $\omega_{j,\alpha\alpha}$ can be determined by the given mode-Grüneisen parameters

$$\gamma_{j,\,\alpha\alpha} = B_0\frac{1}{\omega_{j,\,\alpha\alpha}}\frac{\partial\omega_{j,\,\alpha\alpha}(P)}{\partial P}. \quad (25)$$

The influence of hydrostatic pressure on the high frequency dielectric constants in Eq.(23), following the relation given in Ref.[19], can be rewritten as

$$\frac{\partial\kappa_{\infty,\alpha\alpha}(p)}{\partial p} = -\frac{5(\kappa_{\infty,\alpha\alpha} - 1)}{3B_0}(0.9 - f_i), \quad (26)$$

where f_i is the ionicity of the material under pressure. The dielectric constant of $Al_xGa_{1-x}N$ can be calculated in the SCPA[8]

$$\kappa_{\mathrm{TMC}} = [((1-x)m_{\mathrm{B}}\kappa_{\mathrm{A}}^2 + xm_{\mathrm{A}}\kappa_{\mathrm{B}}^2)(x/m_{\mathrm{A}} + (1-x)/m_{\mathrm{B}})]^{1/2}. \quad (27)$$

4. Numerical results and discussion

We have computed the binding energies of the screened impurity states in a hexagonal GaN/$Al_xGa_{1-x}N$ heterojunction with biaxial and uniaxial free strains by considering hydrostatic pressure effect, with an external electric field applied. All of the parameters used in our computation were given in Ref.[7].

In a free strained wurtzite $GaN/Al_xGa_{1-x}N$ heterojunction with [0001]-orientation, for a given Al concentration $x = 0.3$ and areal electronic density $n_s = 4.0 \times 10^{12}/cm^2$, the results for the binding energies E_B of screened donor-impurity states as functions of impurity position z_0 are illustrated in Fig.1. For comparison, the results of E_B without the screening effect are also shown to indicate that the screening dramatically weakens the attraction of the Coulombic potential, so that E_B decreases significantly. From Fig.1(a), the conspicuous changes of blue and red Stark shifts with z_0 under different electric fields can be seen. A detailed explanation was given in Ref.[7]. It can be found that the screening effect obviously reduces E_B but does not influence the maximum position of E_B. For example, E_B reduces 26.7% for electric field $F = 0$ kV/cm at the maximum point of E_B compared with that without the screening effect. It can also be found that the drop-off of the amplitude increases gradually as z_0 approaches the interface. In Fig.1(b), we give the Stark energy shifts of binding energy as a function of z_0 under different electric fields with and without the screening effect, separately, showing that the screening effect reduces the blue and red shifts dramatically. The weakening of the blue and red shifts, induced by the screening effect, strengthens gradually with the increase of the electric field. This result is consistent with that shown in Fig.1(a).

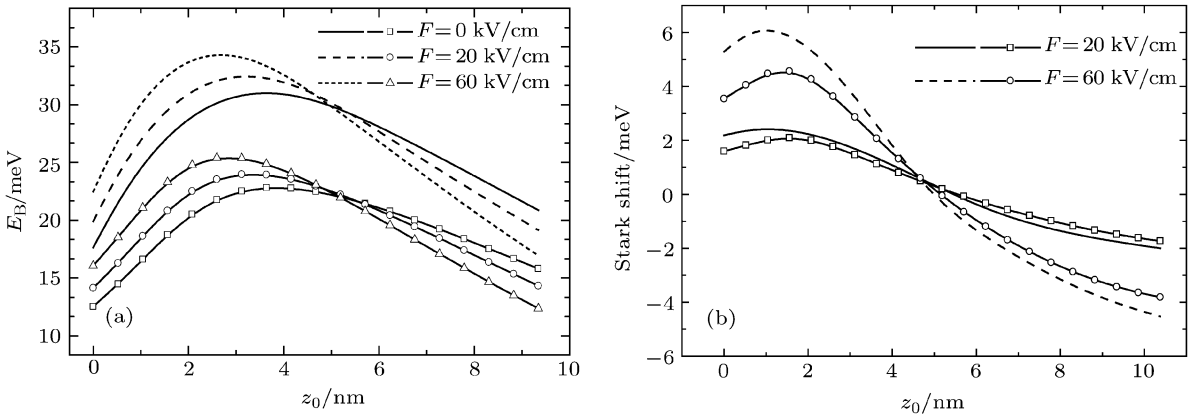


Fig.1. (a) Binding energies and (b) Stark shift of the impurity states in a free strained wurtzite $GaN/Al_xGa_{1-x}N$ heterojunction with [0001]-orientation as functions of impurity position z_0 under different electric fields. The symbol curves and the bare curves are for the results with and without the screening effect, respectively.

The influence of hydrostatic pressure P and the screening effect on E_B is calculated and shown in Fig.2. It can be seen clearly that E_B increases almost linearly as pressure increases, no matter whether screening is present. When P ranges from 0 to 10 GPa, the net increments of E_B for the screened case are 3.075 meV and 2.481 meV, which comprise 13.74% and 11.18% of those for $z_0 = 3$ nm and 5 nm, respectively. A decrease appears as the distance between the impurity and interface increases due to the fact that the comprehensive effect of P on physical parameters influences E_B. On the other hand, the corresponding net increments of E_B for the unscreened case are 4.136 meV and 3.187 meV, which make up 13.31% and 10.63% of those for $z_0 = 3$ nm and 5 nm, respectively. This fact shows that E_B becomes more sensitive to P when the screening effect is taken into consideration.

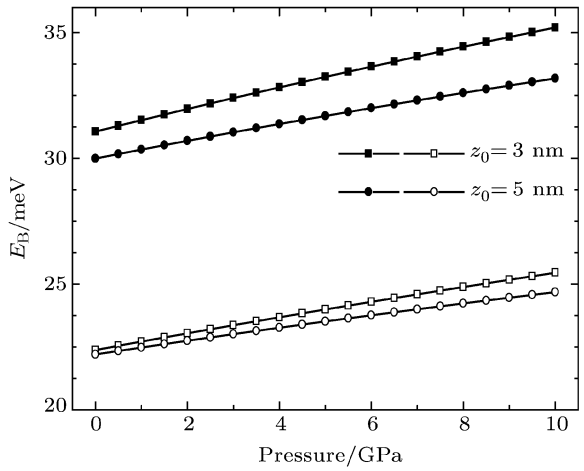


Fig.2. Curves for binding energy as a function of hydrostatic pressure for different impurity positions. The open symbol lines and the solid symbol lines are for the results with and without the screening effect, respectively.

In Fig.3, we display the Stark shifts of E_B with screening effect as a function of the electric field F for different impurity positions. For comparison, the shifts without screening effect are also presented. It can be seen that blue and red shifts monotonically decrease as F increases when the impurity is located at 4 nm and 8 nm, respectively. The influence of screening on the blue shift is more obvious than that on the red shift as F increases, since the screening effect is stronger for a large Coulombic interaction.

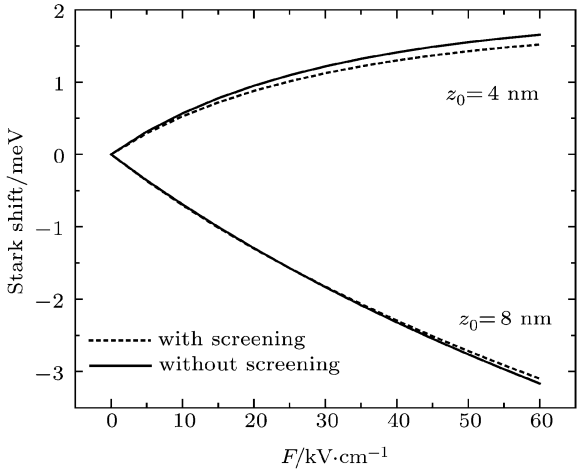


Fig.3. Curves for Stark energy shift of a donor impurity located at two different positions as a function of the electric field for zero pressure.

Figure 4 shows the influence of the Al component x on the Stark effect as a function of electric field for $P = 0$ GPa. Without the screening effect, when $z_0 = 3$ nm and F ranges from 0 to 60 kV/cm, the Stark effects change from 0 meV to 3.136, 3.823, 4.163 meV, for $x = 0.2$, 0.5 and 0.8, respectively. However, the Stark shifts with the screening effect become 2.770, 3.346 and 3.608 meV, which comprise 11.7%, 12.5% and 13.3% in comparison with those without the screening effect, respectively. This indicates that the screening effect weakens the mixture crystal effect, thereby influencing the Stark effect.

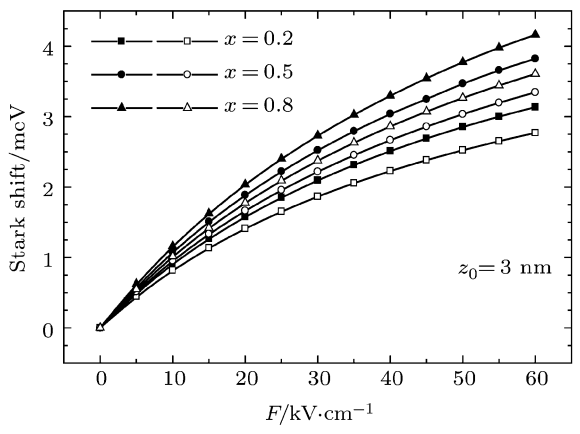


Fig.4. Curves for Stark energy shift of a donor impurity state as a function of electric field for different Al components and $z_0 = 3$ nm. The open symbol lines and the solid symbol lines are for the results with and without the screening effect, respectively.

In Fig.5, we display E_B as a function of n_s for $z_0 = 4$ nm and different values of F. When the value of n_s changes from $0.5\times$ to 10×10^{12}/cm^2, E_B increase 3.665 and 2.946 meV comprising 12.4% and 13.56% of those without and with screening effects, respectively. This is attributed to the fact that the screening effect weakens the Coulombic interaction, thus enhancing the effects of F and energy band bending due to n_s, so that it has a prominent effect on E_B.

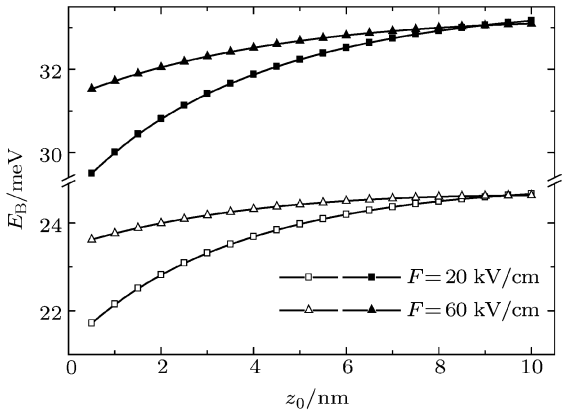


Fig.5. Curves for binding energy as a function of areal electronic density for different electric fields and $z_0 = 4$ nm. The open symbol lines and the solid symbol lines are for the results with and without the screening effect, respectively.

It should be pointed out that the introduction of an external electric field in the heterojunction is also helpful to understand the property of a built-in electric field existing in a real wurtzite GaN/AlGaN heterojunction with finite thickness. The Stark effect in such a system will be studied in the future.

5. Conclusion

We investigated the screening effect on the quantum confined Stark effect of donor impurity states in [0001]-oriented GaN/$Al_xGa_{1-x}N$ heterojunctions with free strain by taking hydrostatic pressure and electric fields into account. The Stark energy shift and the binding energies of the impurity states as functions of the impurity position, the Al component

and the areal electron density are calculated and discussed. It is found that the screening effect reduces both the Stark shift and the binding energy dramatically. For a given impurity position, the change in screened binding energy is more sensitive to the increase of hydrostatic pressure in the presence of the screening effect than that in the absence of the screening effect. It also indicates that the screening effect weakens the Stark shift with the increase of electric field for a given areal electron density. The weakening of the blue and red shifts, induced by the screening effect, strengthens gradually with the increase of the electric field. Furthermore, the screening effect weakens the mixture crystal effect, thereby influencing the Stark effect.

References

[1] Jogai B 1998 *Phys. Rev.* B **57** 2382
[2] Pokatilov E P, Nika D L, Fomin V M and Devreese J T 2008 *Phys. Rev.* B **77** 125328
[3] Ha S H and Ban S L 2008 *J. Phys: Condens Matter* **20** 085218
[4] Łepkowski S P 2008 *Phys. Rev.* B **77** 155327
[5] Wagner J M and Bechstedt F 2000 *Phys. Rev.* B **62** 4526
[6] Zhang M and Ban S L 2008 *Acta Phys. Sin.* **57** 4459 (in Chinese)
[7] Zhang M and Ban S L 2009 *Chin. Phys.* B **18** 4449
[8] Ban S L and Hasbun J E 1999 *Eur. Phys. J.* B **8** 453
[9] Ando T, Fowler A B and Stem F 1982 *Rev. Mod. Phys.* **54** 437
[10] Brum J A, Barstard G and Guillemot C 1984 *Phys. Rev.* B **30** 905
[11] Ban S L and Hasbun J E 1999 *Solid State Commun.* **109** 93
[12] Wagner J M and Bechstedt F 2002 *Phys. Rev.* B **66** 115202
[13] Łepkowski S P 2007 *Phys. Rev.* B **75** 195303
[14] Perlin P, Mattos L, Shapiro N A, Kruger J, Wong W S, Sands T, Cheung N W and Weber E R 1999 *J. Appl. Phys.* **85** 2385
[15] Shan W, Hauenstein R J, Fischer A J, Song J J, Perry W G, Bremser M D, Davis R F and Goldenberg B 1996 *Phys. Rev.* B **54** 13460
[16] Christensen N E and Gorczyca I 1994 *Phys. Rev.* B **50** 4397
[17] Nardelli M B, Rapcewicz K and Bernholc J 1997 *Phys. Rev.* B **55** R7323
[18] Ting D Z Y and Chang Y C 1987 *Phys. Rev.* B **36** 4359
[19] Goñi A R, Syassen K and Cardona M 1990 *Phys. Rev.* B **41** 10104